Article

# Intervalence Near-IR Spectra of Delocalized Dinitroaromatic Radical Anions

Stephen F. Nelsen, Asgeir E. Konradsson, Michael N. Weaver, and Joo P. Telo

*J. Am. Chem. Soc.*, **2003**, 125 (41), 12493-12501• DOI: 10.1021/ja036066m • Publication Date (Web): 18 September 2003



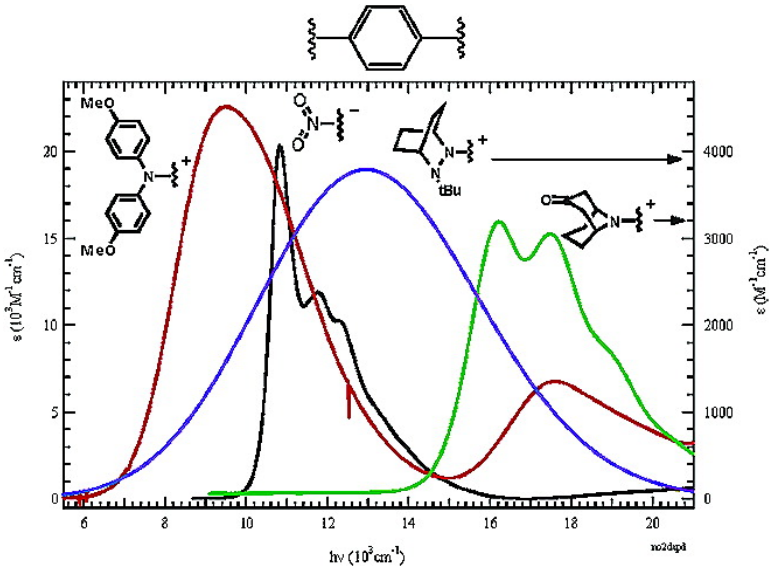


## More About This Article

Additional resources and features associated with this article are available within the HTML version:

- Supporting Information
- Links to the 7 articles that cite this article, as of the time of this article download
- Access to high resolution figures
- Links to articles and content related to this article
- Copyright permission to reproduce figures and/or text from this article

View the Full Text HTML

J|A|C|S
ARTICLES
Published on Web 09/18/2003

# Intervalence Near-IR Spectra of Delocalized Dinitroaromatic Radical Anions

Stephen F. Nelsen,*,† Asgeir E. Konradsson,† Michael N. Weaver,† and João P. Telo*,‡

*Contribution from the Department of Chemistry, University of Wisconsin, 1101 University Avenue, Madison Wisconsin 53706-1396, and Instituto Superior Técnico, Química Orgânica, Av. Rovisco Pais, 1049-001 Lisboa, Portugal*

Received May 11, 2003; E-mail: nelsen@chem.wisc.edu

***Abstract:*** The Class III (delocalized) intervalence radical anions of 1,4-dinitrobenzene, 2,6-dinitronaphthalene, 2,6-dinitroanthracene, 9,9-dimethyl-2,7-dinitrofluorene, 4,4′-dinitrobiphenyl, and 1,5-dinitronaphthalene show charge-transfer bands in their near-IR spectra. The dinitroaromatic radical anions have comparable but slightly larger electronic interactions ($H_{ab}$ values) through the same aromatic bridges as do the corresponding dianisylamino-substituted radical cations. $H_{ab}$ values range from 5410 $cm^{-1}$ (1,4-dinitrobenzene) to 3400 $cm^{-1}$ (9,9-dimethyl-2,7-dinitrofluorene), decreasing as the number of bonds between the nitro groups increases, except for the 1,5-dinitronaphthalene radical-anion, which has a coupling similar to that of 9,9-dimethyl-2,7-dinitrofluorene. All charge-transfer bands show vibrational fine structure. The vertical excitation energies ($\lambda_v$) were estimated from the vibrational components, obtained by simulation of the entire band. The large $2H_{ab}/\lambda_v$ values confirm these radicals to be Class III delocalized mixed-valence species. Analysis using Cave and Newton's generalized Mulliken−Hush theory relating the transition dipole moment to the distance on the diabatic surfaces suggests that the electron-transfer distance on the diabatic surfaces, $d_{ab}$, is only 26−40% of the nitrogen-to-nitrogen distance, which implies that something may be wrong with our analysis.

## Introduction

Interest in the question of charge localization versus delocalization in dinitroaromatic anions began with early ESR studies showing that 1,3-dinitrobenzene radical anion has spin localized on one nitro group when prepared by alkali metal reduction in an ether solvent,[1] but the nitro groups appeared equivalent when it was prepared by electrochemical reduction.[2] Intense study by many groups for a decade showed that the rate of electron exchange between the nitro groups was very sensitive to conditions and led to general agreement that interactions of the radical anion with solvent and counterion were responsible for the charge localization.[3] More recently, the intramolecular electron-transfer rate constants for these and many analogous systems have been measured more accurately,[4] and it was shown by Hosoi and co-workers that reducing with excess [222]-cryptand

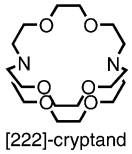

[222]-cryptand

and sodium in DMF[5] gives about an order of magnitude higher rate constant than electrochemical reduction,[4] so that even ion pairing with $Bu_4N^+$ in polar solvents causes an easily detectable effect on the electron transfer (ET) rate constants.

Surprisingly, although it is now obvious that these systems should be considered nitro-centered intervalence (IV) compounds and hence their optical spectra will be revealing about their ET properties, we have seen no discussion of the near-IR spectra of dinitroaromatic radical anions. We consider the delocalized systems in this work. IV compounds have two charge-bearing units (**M**), connected by a bridge (**B**), and ones that have an electronic interaction through the bridge exhibit an IV-band in their optical spectra. Symmetrical, localized IV compounds (designated as Robin−Day Class II systems)[6] that may be symbolized as $\mathbf{M}-\mathbf{B}-\mathbf{M}^+$ or $\mathbf{M}-\mathbf{B}-\mathbf{M}^-$ provide the simplest ET systems to interpret. The Marcus−Hush two-state model[7] provides a remarkably simple way of considering their optical spectra. As indicated at the left of Figure 1, for a localized compound the transition energy at the band maximum

† University of Wisconsin.
‡ Instituto Superior Técnico.

(1) (a) Ward, R. L. *J. Chem. Phys.* **1960**, *32*, 410. (b) Ward, R. L. *J. Am. Chem. Soc.* **1961**, *83*, 1296. (c) Ward, R. L. *J. Chem. Phys.* **1962**, *37*, 1405.
(2) (a) Maki, A. H.; Geske, D. H. *J. Chem. Phys.* **1960**, *33*, 825. (b) Maki, A. H.; Geske, D. H. *J. Am. Chem. Soc.* **1961**, *83*, 1852. (c) Harriman, J. E.; Maki, A. H. *J. Chem. Phys.* **1963**, *39*, 778.
(3) Gutch, J. W.; Waters, W. A.; Symons, M. C. R. *J. Chem. Soc. B* **1970**, 1261.
(4) (a) Grampp, G.; Shohoji, M. C. B. L.; Herold, B. J. *Ber. Bunsen-Ges. Phys. Chem.* **1989**, *93*, 580. (b) Grampp, G.; Shohoji, M. C. B. L.; Herold, B. J.; Steenken, S. *Ber. Bunsen-Ges. Phys. Chem.* **1990**, *94*, 1507. (c) Telo, J. P.; Shohoji, M. C. B. L.; Herold, B. J.; Grampp, G. *J. Chem. Soc., Faraday Trans.* **1992**, *88*, 47. (d) Telo, J. P.; Shohoji, M. C. B. L. *Ber. Bunsen-Ges. Phys. Chem.* **1994**, *98*, 172.
(5) Hosoi, H.; Mori, Y.; Masuda, Y. *Chem. Lett.* **1998**, 177.
(6) Robin, M.; Day, P. *Adv. Inorg. Radiochem.* **1967**, *10*, 247.

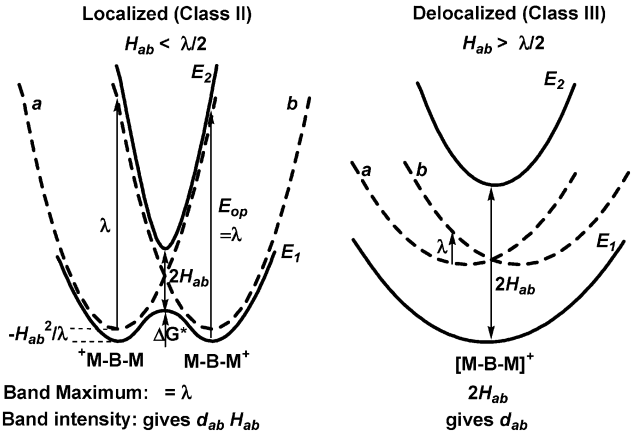


***Figure 1.*** Comparison of IV charge-transfer band interpretation for localized and delocalized IV compounds.

($E_{op}$) on the adiabatic surfaces (solid lines) is the separation between the ground ($E_1$) and excited state ($E_2$) energy surfaces, and equals Marcus's vertical reorganization energy $\lambda$, the vertical gap between the minimum of one diabatic surface and the other (the dashed parabolas marked *a* and *b*). Hush suggested how to experimentally determine the electronic coupling between the **M** units, $H_{ab}$, that allows determining the electron-transfer barrier, $\Delta G^*$ (when the ET distance $d_{ab}$ is known).[7a] If $2H_{ab}$ exceeds $\lambda$, the interpretation of the IV charge-transfer band is very different (right side of Figure 1). The lower-energy surface then has a single minimum, the compound is charge-delocalized (Robin−Day Class III), and $E_{op}$ measures $2H_{ab}$ instead of $\lambda$. We believe it was Cave and Newton who first pointed out in their generalized Mulliken−Hush (GMH) theory that band intensity for Class III compounds becomes a measure of $d_{ab}$.[8] In this work we discuss the IV absorption bands of six delocalized dinitroaromatic anions having the five-, seven-, and nine-bond aromatic bridges shown below,

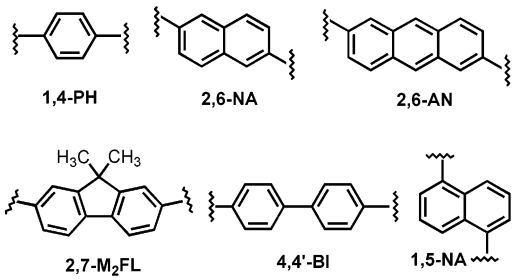


and compare their optically derived ET parameters with an IV radical anion having 2,2-difluoro-1,3,2-(2H)-dioxaborine (**Db**) units, and radical cations having dianisylamino (**Da**), 3-keto-azabicycl[3.3.0]non-9-yl (**k33N**), and 2-*tert*-butyl-2,3-diazabicyclo-[2.2.2]oct-3-yl (**Hy**) charge-bearing units.

## Results

The optical absorption spectra of dinitroaromatic radical anions were recorded in DMF after reduction with sodium amalgam in the presence of a large excess of the cryptand

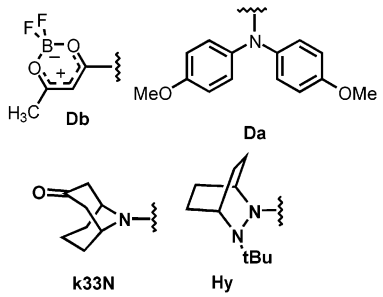


illustrated above, the conditions shown by Hosoi and co-workers to avoid tight ion pairing.[5]

Localized IV compounds have their low-energy optical transition to a steeply sloping region of the upper adiabatic surface (Figure 1), ensuring that the absorption band will be very broad, and precluding the resolution of vibrational fine structure. Delocalized IV compounds have a minimum vertical from the ground-state minimum, and can show narrow enough lines to resolve vibrational fine structure. All of the compounds discussed here have partially resolved vibrational fine structure, requiring that they are delocalized (Class III) systems. Figure 2 compares the low-energy region spectra for the **1,4-PH**-bridged nitro-centered radical anion with those for the three **1,4-PH**-bridged radical cations. The **1,4-Da$_2$PH**$^+$ spectrum was taken in methylene chloride[9,10] and the **1,4-(k33N)$_2$PH**$^+$ and **1,4-Hy$_2$PH**$^+$ spectra in acetonitrile,[11] but solvent effects on delocalized IV compound optical spectra are small.[12] The **NO$_2$**-substituted radical anion spectrum shows the resolution of vibrational structure, as does the **k33N**- substituted cation.

The effect of changing bridge size on three of these **NO$_2$**-centered radical anions is shown in Figure 3. As expected, $E_{op}$ decreases as bridge size increases because $H_{ab}$ will decrease. All three bands show rather distinct vibrational fine structure, with components showing maxima at ~1450, 1550, and 1520 $cm^{-1}$ higher energy than the 0,0 band as ring size increases, of relative $\epsilon_{max}$ ~0.50, 0.36, 0.36. An intermediate maximum occurs for the smaller systems but is not noticeable for the **2,6-AN**-bridged compound. Optical data, transition dipole moments ($\mu_{12}$), and related information are summarized in Table 1.

Figure 4 compares the optical spectra of the IV radical anions of the three nine-bond bridged compounds studied, with **2,6-AN, 2,7-M$_2$FL**, and **4,4′-BI** bridges. The spectrum is noticeably broader for the **2,7-M$_2$FL**-bridged compound and broader yet for the **4,4′-BI**-bridged one. Figure 5 compares the optical spectra for the 1,5- and 2,6-naphthalene-bridged radical anions. Despite a shorter distance and fewer connecting bonds, $H_{ab}$ is smaller for the former compound, which certainly needs explaining.

The transition dipoles ($\mu_{12}$) in Table 1 were calculated as described in the Experimental Section and converted to $d_{ab}$ using the generalized Mulliken−Hush formula $d_{ab} = 2\mu_{12}/e$ which arises because the electron-transfer distance on the ground-state adiabatic surface, $d_{12}$, is zero for a delocalized compound.[8b]

(7) (a) Hush, N. S. *Prog. Inorg. Chem.* **1967**, *8*, 391. (b) Hush, N. S. *Coord. Chem. Rev.* **1985**, *64*, 135. (c) Marcus, R. A.; Sutin, N. *Biochim. Biophys. Acta* **1985**, *811*, 265. (d) Sutin, N. *Prog. Inorg. Chem.* **1983**, *30*, 441.

(8) (a) Cave, R. J.; Newton, M. D. *J. Chem. Phys.* **1997**, *106*, 9213. (b) Obtained from $|\Delta\mu_{ab}| = [(\Delta\mu_{12})^2 + 4(\Delta\mu_{12})^2]^{1/2}$ using $\Delta\mu(D) = 4.8032d$ (Å).

(9) Lambert, C.; Nöll, G. *J. Am. Chem. Soc.* **1999**, *121*, 8434.

(10) Nelsen, S. F.; Konradsson, A. E.; Luo, Y. Kim, K. Y.; Blackstock, S. C., submitted for publication, reassigns the **Da$_2$Ar**$^+$ species considered here as delocalized; Lambert and Nöll thought it was localized.[9]

(11) Bailey, S.; Zink, J. I.; Nelsen, S. F. *J. Am. Chem. Soc.* **2003**, *125*, 5939.

(12) Nelsen, S. F.; Tran, H. Q. *J. Phys. Chem. A* **1999**, *103*, 8139.

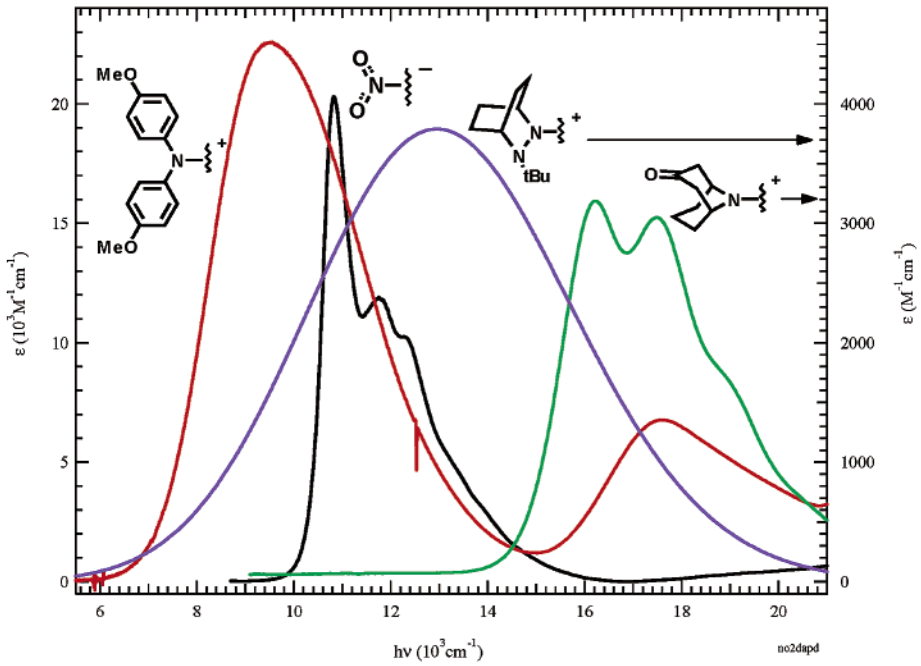


***Figure 2.*** Comparison of $\epsilon$ vs $h\nu$ for four **PH**-bridged IV compounds. The **Da**- and **$NO_2$**-bridged species are plotted versus the left $\epsilon$ axis, and the **Hy**- and **k33N**-bridged on the right one, which is expanded by a factor of 5 so that all four spectra may be clearly seen.

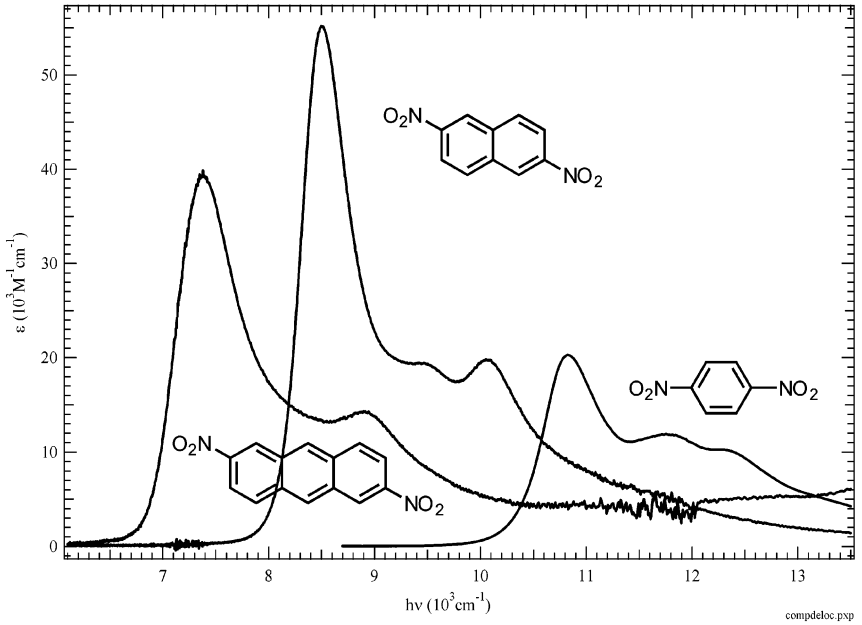


***Figure 3.*** Comparison of the absorption spectra of the **1,4-PH**, **2,6-NA**, and **2,6-AN**-bridged dinitroaromatic radical anions at room temperature in DMF.

***Table 1.*** Comparison of IV Region Optical Absorption Parameters for Delocalized Dinitroaromatic Radical Anions in DMF

| bridge | $E_{op}$ ($cm^{-1}$) | $\epsilon_{max}$ ($M^{-1}cm^{-1}$) | $\mu_{12}$ (Debye) | $d_{ab}$ (Å) | $d_{NN}$ (Å)[a] | $d_{ab}/d_{NN}$ |
|---|---|---|---|---|---|---|
| 1,4-PH | 10820 | 20300 | 4.66 | 1.94 | 5.60 | 0.35 |
| 2,6-NA | 8500 | 55200 | 7.60 | 3.15 | 7.81 | 0.40 |
| 2,6-AN | 7380 | 39900 | 6.85 | 2.85 | 10.26 | 0.28 |
| 2,7-$M_2$−FL | 6790 | 16470 | 5.7−5.9 | 2.4−2.5 | 9.75 | 0.25−0.26 |
| 4,4′-BI | 6900 | 9920 | 6.09 | 2.54 | 9.91 | 0.26 |
| 1,5-NA | 6800 | 6380 | 4.02 | 1.68 | 6.34 | 0.26 |

[a] From UHF/AM1 calculations.

## Discussion

***$H_{ab}$* Values.** The bridge size effect on $H_{ab} = E_{op}/2$, displayed versus the number of bonds between the nitrogens for the Class III **$NO_2$**-centered anions is shown in Figure 6, which compares them with the Class III **(k33N)$_2$Ar$^+$** and **Da$_2$Ar$^+$** cations[10] as well as the Class II **Hy$_2$Ar$^+$** radical cations,[13] for which the $H_{ab}$ values were obtained from band intensities. The approximately linear log($H_{ab}$) versus number of bonds (usually stated as "distance") behavior that everyone expects[7] is observed, except for the **1,5-NA** bridge, as discussed below. It should be noted that the substituents **M** must be attached to the bridge in a "Kekule" substitution pattern, as they are here, for this to occur. The bridges considered here lead to large $H_{ab}$ values

(13) (a) Nelsen, S. F.; Ismagilov, R. F.; Powell, D. R. *J. Am. Chem. Soc.* **1997**, *119*, 10213. (b) Nelsen, S. F.; Ismagilov, R. F.; Gentile, K. E.; Powell, D. R. *J. Am. Chem. Soc.* **1999**, *121*, 7108. (c) Nelsen, S. F.; Trieber, D. A. II; Ismagilov, R. F.; Teki, Y. *J. Am. Chem. Soc.* **2001**, *123*, 5684.

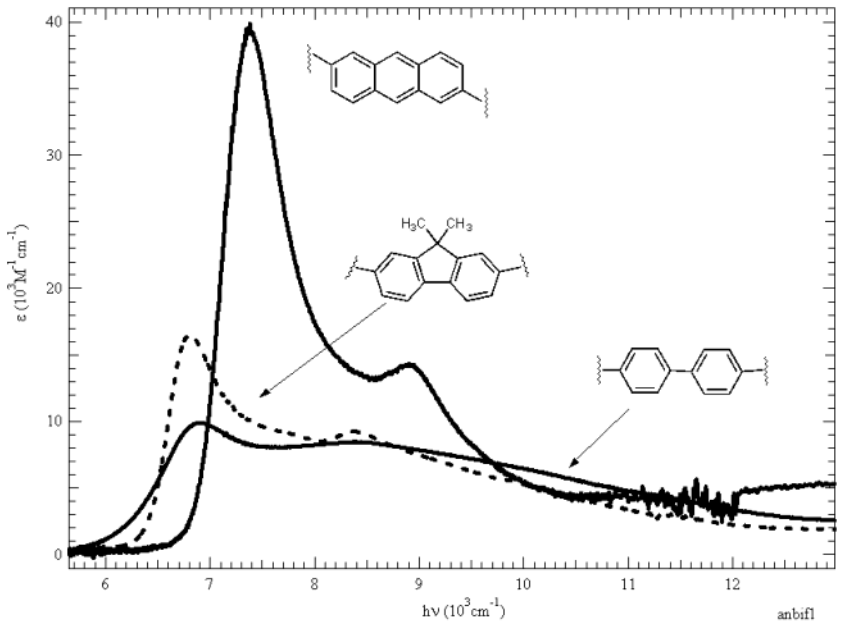


***Figure 4.*** Optical spectra for the nine-bond-bridged dinitroaryl radical anions bridged by 2,6-anthracenediyl, 9,9-dimethyl-2,7-fluorenediyl, and 4,4′-biphenyldiyl groups at room temperature in DMF.

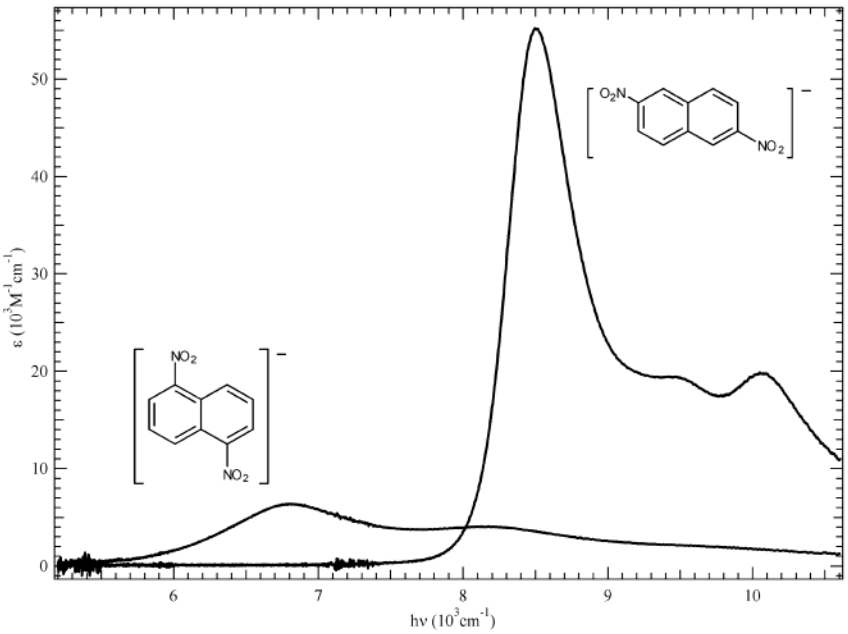


***Figure 5.*** Comparison of the optical spectra for the 1,5- and 2,6-dinitronaphthalene radical anions at room temperature in DMF.

because the second **M** substituent is attached at a carbon that formally bears a large coefficient in the monosubstituted radical ion, $[\mathbf{M}-\mathbf{Ar}]^{\bullet(+/-)}$. This is called a Kekule substitution pattern by people considering magnetic interactions between spin-bearing centers[14] because, for example, the formally "**•OArO•**" compounds with these bridges are quinones, with all electrons paired that have large energy gaps to diradical excited states. In contrast, non-Kekule substitution pattern examples having **1,3-PH** and **2,7-NA** bridges, where the second **O•** is attached at a carbon at a Hückel node in $[\mathbf{O}^{\bullet-}\mathbf{Ar}]$, have to be written with diradical Kekule structures (or small rings), have tiny electronic interactions through the bridge, and are ground-state triplet species. We shall discuss non-Kekule substitution pattern $\mathbf{(NO_2)_2Ar}^{\bullet-}$ IV compounds in future work.

It will be noted from Figure 6 that something in addition to distance even for Kekule substitution pattern compounds is clearly significantly involved in determining $H_{ab}$, because the five-bond **1,5-NA** bridge not only leads to a smaller coupling than the **2,6-NA** one, it is also smaller than all three of the nine-bond bridge examples studied. A similar pattern is calculated to occur even for the untwisted diamino radical cations,[15] and the low coupling for the **1,5-NA** bridge seems most easily considered by considering the related quinones. The order of the couplings in the dinitroaromatics may be noted to be that obtained by considering the **1,5-NA**-bridged compound as having 11 bonds between the nitrogens, that is by counting around

(14) Rajca, A. *Chem. Rev.* **1994**, *94*, 871.

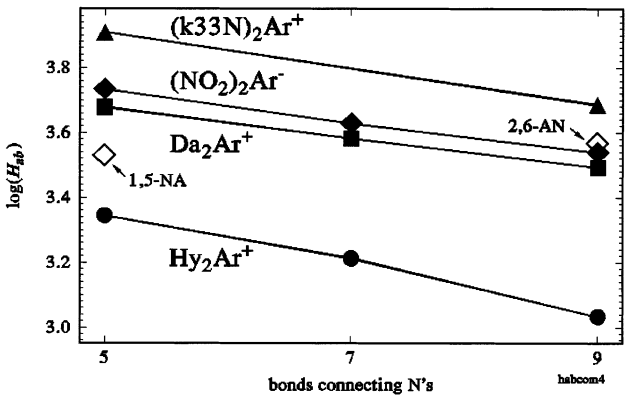


***Figure 6.*** Plot of log($H_{ab}$) versus number of connecting bonds for organic IV compounds: The five-bond bridge is **1,4-PH**, the seven-bond bridge **2,6-NA**, and the nine-bond bridge **4,4′-BI**, except as noted for the two dinitro compounds shown as open diamonds.

the alternating double and single bond array instead of across the shorter distance of the single-bonded five-bond pathway.

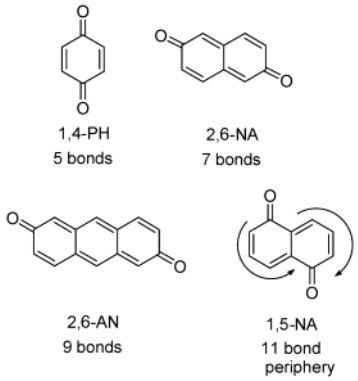


Each carbonyl group in the 1,5-isomer is substituted meta (to the other carbonyl group) on the six-membered ring to which it is attached, which is a non-Kekule substitution pattern that leads to small coupling. The five-bond shortest pathway is not functional for coupling and is replaced by the 11-bond Kekule pathway. We also show a plot of the log($H_{ab}$) values versus this "bonds" count as Figure 7. We note that the plot is significantly curved, so log($H_{ab}$) is not linear with the number of bonds even for the largest $H_{ab}$ benzene, naphthalene, and anthracene examples. The logarithmic dependence upon distance was derived for bridges that consist of repeating units. Although double and triple bonds, 1,4-benzene diyl units, and their combinations do lead to nearly linear plots of log($H_{ab}$) versus number of bonds or distance, even this linear fused ring aromatic series leads to quite noticeable deviations from a linear log relationship.

A notable aspect of Figure 6 is that **(NO$_2$)$_2$Ar**$^-$ and **Da$_2$Ar**$^+$ lead to such similar $H_{ab}$ values. The nitro and dianisylamine charge-bearing units have almost nothing in common structurally, but the two-state model does not consider **M** group structure and should allow quantitative evaluation of the charge-bearing unit electronic interactions of these structurally dissimilar compounds. **Da** and **NO$_2$** groups do share one structural feature: they have a single nitrogen attached to the aromatic bridge that bears much of the spin but has substantial charge delocalization onto the other groups attached to nitrogen.

(15) Unpublished results of semiempirical AM1 calculations.

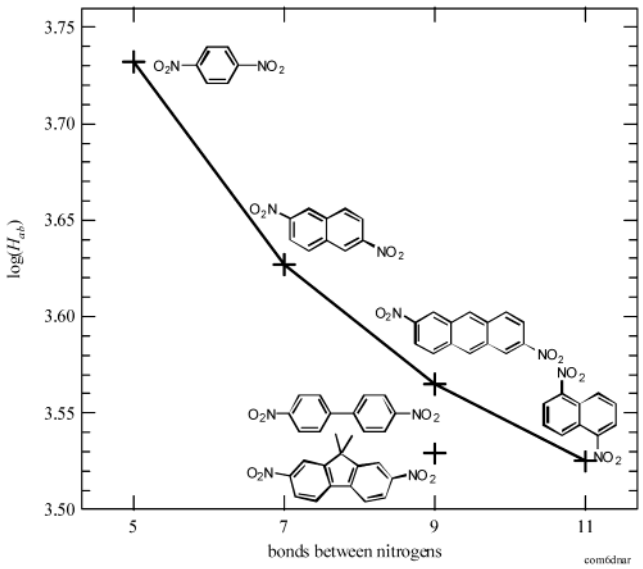


***Figure 7.*** Plot of log($H_{ab}$) versus the number of bonds between the nitrogens, counted around the periphery for the 1,5-naphthalene derivative, for delocalized intervalene dinitroaromatic anions.

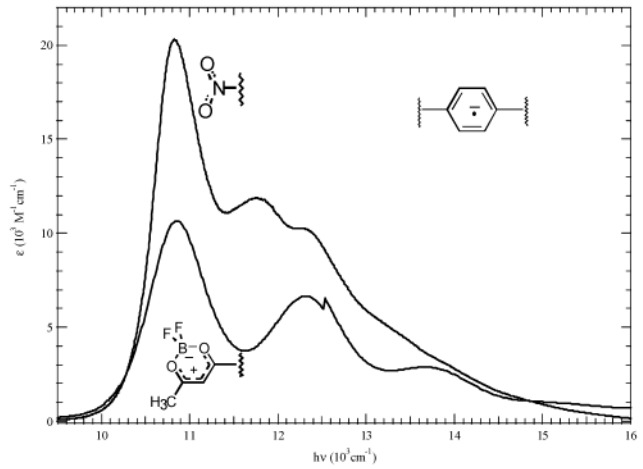


***Figure 8.*** Comparison of the PH-bridged $NO_2^-$ and difluorodioxaborine-centered radical anions.

This is seen to be enough similarity to give them comparable $H_{ab}$ values, although the **(NO$_2$)$_2$Ar**$^-$ compounds have slightly larger ones for all three bridge sizes studied. An even closer congruence of $H_{ab}$ values for **PH**-bridged IV compounds occurs for **1,4-(NO$_2$)$_2$Ar**$^-$ and the recently reported difluorodioxaborine radical anion **Db$_2$PH**$^-$ (studied in acetonitrile);[16] their optical spectra are compared in Figure 8. Although there is even less structural similarity in the charge-bearing units than between **Da** and **NO$_2$** (which are at least both nitrogen-centered), the compounds in Figure 8 have $H_{ab}$ values that only differ by 25 cm$^{-1}$ (0.5%), with that for **(NO$_2$)$_2$PH**$^-$ in DMF being slightly smaller. Figure 2 emphasizes, however, that $H_{ab}$ is not exclusively determined by the bridge; examples are shown that differ by over 3300 cm$^{-1}$.

It will be noted from Table 1 that $H_{ab}$ is about 55 cm$^{-1}$ smaller for the 9,9-dimethyl-2,7-dimethylfluorenediyl-bridged compound than for the 4,4′-biphenyldiyl-bridged one (**FL**/**BI**

(16) (a) Risko, C.; Barlow, S.; Coropceanu, V.; Halik, M.; Bredas, J.-L.; Marder, S. R. *Chem. Commun.* **2003**, 194. (b) We thank Professor Barlow for providing the optical spectrum of **Db$_2$PH**$^-$ for determination of $\mu_{12}$ and hence $d_{ab}$.

ratio 0.98). Since the fluorenediyl ring prevents twisting about the central bond and $H_{ab}$ is expected to be proportional to the cosine of the twist angle at this bond, one might have expected $H_{ab}$ to be larger for the fluorenediyl compound. In fact, $H_{ab}$ is signficantly larger for the fluorenediyl-bridged **Hy**-centered radical cation than for the biphenyldiyl-bridged one (estimated **FL**/**BI** ratio 1.13).[13b] In principle, all the charge-bearing units (CBU) and bridge orbital interactions will contribute to $H_{ab}$.[17] The total $H_{ab}$ is the sum of all the contributions. However, these contributions are weighted by $1/\Delta E$, the energy difference between each CBU and bridge orbital involved. The smallest energy gap contribution therefore dominates $H_{ab}$, and Newton has suggested designating systems such as $\mathbf{Hy_2Ar^+}$, that have the CBU SOMO, bridge HOMO energy gap smallest as "hole transfer" ones, and systems such as the $\mathbf{(NO_2)_2Ar^-}$ ones considered here, which have the CBU SOMO, bridge LUMO energy gap the smallest, as "electron transfer" ones.

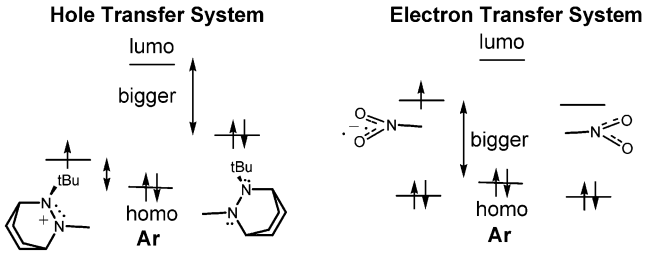


Apparently the change in the dominant ring orbital for these systems is more than enough to offset the effect of twisting at the central bond.

**Electron-Transfer Distance on the Diabatic Surfaces ($d_{ab}$).** According to the generalized Mulliken−Hush theory of Cave and Newton,[8] when a compound is delocalized, the electron-transfer distance on the adiabatic surfaces ($d_{12}$) drops to zero; therefore, the electron-transfer distance on the diabatic surfaces ($d_{ab}$) may be directly obtained from the transition dipole moment $\mu_{12}$ using $d_{ab}$ (Å) = $2\mu_{12}$(Debye)/4.8032. Values of $d_{ab}$ determined by this method are included in Table 1. Also listed is the distance between the nitrogen atoms that are bonded to the bridge ($d_{NN}$), which is the "edge-to-edge" distance between the charge-bearing units, that has very often been used as $d_{ab}$ in calculating $H_{ab}$ values for localized IV compounds.[9] The $d_{ab}$ values for **1,4-PH**-bridged compounds with the charge-bearing units under discussion are compared visually in Figure 9. We note that $d_{ab}$ for the same bridge is obviously dependent upon the $H_{ab}$ that the charge-bearing unit causes, decreasing significantly as $H_{ab}$ increases. Even for the charge-localized Class II **Hy**-centered compound, where the $H_{ab}$ value is significantly smaller, $d_{ab}$ is significantly smaller than $d_{NN}$,[18] and the $d_{ab}$ values for delocalized compounds obtained from $\mu_{12}$ very clearly drop as $H_{ab}$ increases.

As emphasized in our discussion of the delocalized **Da**-centered compounds,[10] $d_{ab}$ depends on the structure of the charge-bearing units, and the use of $d_{NN}$ as a measure of $d_{ab}$ leads to large errors when used for organic compounds. It seems obvious from this plot that $d_{NN}$ would only be an appropriate ET distance in the limit of small $H_{ab}$, which is rarely the case for IV compounds. Note also that despite the similarity of $H_{ab}$ for $\mathbf{Da_2PH^+}$ and $\mathbf{(NO_2)_2PH^-}$, the $d_{ab}$ value obtained for the latter is significantly smaller. For the other anion considered here, $\mathbf{Db_2PH^-}$, the $d_{ab}$ value obtained is 1.6 Å (it would rise to 1.8 Å if $\epsilon_{max}$ for this rather unstable species had been underestimated by 20%) and even smaller than that for $\mathbf{(NO_2)_2PH^-}$. The lower values for the nitro and difluoro-dioxaborine-centered compounds are consistent with anions showing smaller $d_{ab}$ values than cations, although why this might happen is not clear. From the data of Table 1, not only is $d_{ab}$ a rather small fraction of $d_{NN}$, but also the values obtained are smaller for all three nine-bond-bridged dinitro compounds (**4,4′-BI** and **2,6-AN)** than for the 7-bond **2,6-NA**-bridged one. Such an inversion of $d_{ab}$ as the bridge size increases does not occur for the **Da**-centered cations.[10] Although the anions studied here are less stable than the previously studied cations and could not be purified by crystallization, the $\epsilon_{max}$ values obtained for different experiments are reproducible to about 10%, thus, we do not believe that either the large deviation for the nitro compound point in Figure 9 or the anomalously small values for the nine-bond-bridged compounds are caused by experimental error in calculating $d_{ab}$ (which would be caused by errors in the concentration). One might question whether the concept of the two-state model $d_{ab}$ value for these delocalized compounds is especially useful, but the quite remarkable success of the two-state model for quantitatively interpreting electron-transfer rate constants for Class II systems[13] indicates that it works rather well, and these are the results it gives for delocalized systems.

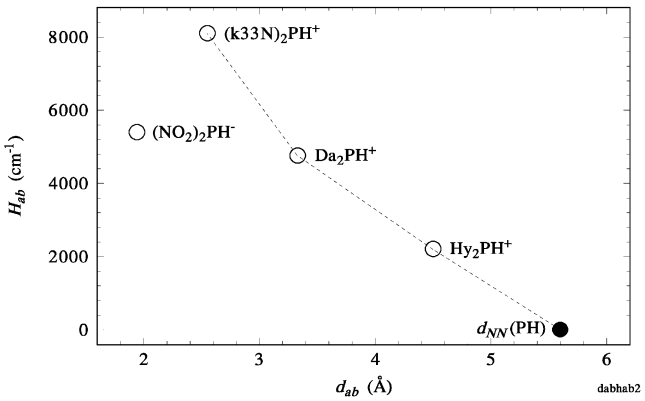


***Figure 9.*** Comparison of the relationship between $d_{ab}$ and $H_{ab}$ for **1,4-PH**-bridged IV compounds.

**Intervalence Band Vibrational Structure and $\lambda_v$.** The line widths of the four 1,4-**PH**-bridged IV compounds shown in Figure 2 are very different. The localized $\mathbf{Hy_2PH^+}$ has by far the largest line width and the nearly Gaussian shape (high-energy side only slightly broader than the low-energy side) of most other Class II IV compounds. $\mathbf{Da_2PH^+}$ has a narrower band that is considerably broader on the high-energy side than the low-energy side[9] but has no vibrational structure resolved. As discussed in detail elsewhere, although $\mathbf{Da_2PH^+}$ is delocalized, it has a $2H_{ab}/\lambda$ ratio not very far from the Class III/II borderline value of 1. For example, the nine-bond $\mathbf{Da_2}$**-4,4′-BI**-bridged species appears to be delocalized in methylene chloride but localized in acetonitrile.[10] The more strongly delocalized **k33N**- and $\mathbf{NO_2}$-centered species show partially resolved vibrational structure, although the latter clearly has narrower lines. The band resolution is slightly better for $\mathbf{Db_2PH^-}$ than for $\mathbf{(NO_2)_2PH^-}$

(17) Newton, M. B. *Chem. Rev.* **1991**, *91*, 767.
(18) Nelsen, S. F.; Newton, M. D. *J. Phys. Chem. A* **2000**, *104*, 10023.

***Table 2.*** Comparison of the **$(NO_2)_2$-PH$^-$** IV Band Simulation Parameters with a Density Functional Theory Vibrational Frequency Calculation

| simulation ($\Gamma$=556 cm$^{-1}$) | | | B3LYP/6-31+G* calculation | | | |
|---|---|---|---|---|---|---|
| $h\nu_q$ (cm$^{-1}$) | $\Delta_q$ | $\lambda_v$(q) (cm$^{-1}$) | vibration number | frequency (cm$^{-1}$) | rel. Raman intensity | description of vibration |
| 310 | 0.58 | 52.1 | 7 | 306 | 0.04 | $CNO_2$,$CNO_2$ stretch |
| | | | 12 | 557 | 0.001 | $NO_2$ in plane rock |
| 590 | 0.79 | 184.1 | 13 | 623 | 0.003 | chair deformation of ring |
| | | | 16 | 695 | 0.03 | O's out + $C_2C_6$ in |
| 990 | 0.86 | 366.1 | 21 | 847 | 0.07 | O's out + $C_2C_6$ out |
| | | | 25 | 1119 | 0.59 | C−H bend + $C_{1,4}$ stretch |
| 1460 | 0.53 | 205.1 | 32 | 1394 | 0.23 | $C_{1,4}$−N stretch |
| 1640 | 0.47 | 181.1 | 38 | 1639 | 1.00 | $C_2$−$C_3$ stretch |
| (3200) | 0.21 | (64.0) | 42 | 3246 | 0.05 | CH stretch + $C_6$ breathe |

(see Figure 8) with separation of the maximum from the features of largest separation of 1460 and 1420 cm$^{-1}$, respectively.

Brédas and co-workers have recently estimated vibrational reorganizational energies ($\lambda_v$) for electron transfers by analysis of spectra that show partial resolution of vibrational fine structure, including the photoelectron spectra of anthracene, tetracene, and pentacene,[19] and the absorption spectrum of **$Db_2PH^-$**.[16] A problem with doing this is that such spectra can be fit with few modes (Brédas and co-workers used three for the compounds mentioned), but many more are probably involved, quite possibly leading to underestimation of the reorganization energy. Brédas and workers' $\lambda_v$ estimates from vibrational analysis of the photoelectron spectra of acenes are 51−59% as large as the calculated values.[19] Our resonance Raman study of **$(k33N)_2PH^+$** identified nine symmetrical vibrational modes (each having significant calculated nonresonance Raman intensity) contributing to its IV band and gave the experimental $\Delta$ values for each which allow accurate calculation of the $\lambda_v$ value.[11] Resonance Raman data are not available for the much less stable dinitroaromatic radical anions studied here. Nevertheless, obtaining a fit to an absorption spectrum that shows vibrational structure places limits on the size of $\lambda_v$ that is probable, and we analyze the spectrum of the dinitro compounds studied here to estimate $\lambda_v$, allowing estimation of $2H_{ab}/\lambda_v$.

In the absence of resonance Raman data, only a simplified fitting treatment is appropriate, because both the frequencies and their dimensionless displacements ($\Delta_q$) must be assumed. We used Zink's simulation program abs/emis/Raman (see Experimental Section) that assumes pure harmonic oscillators, no change in force constant between the ground and excited states, and neither vibrational nor electronic state coupling, assumptions that do not have to be made when resonance Raman excitation profiles are available.[11,20] Using these assumptions, the dimensionless displacement for a mode is related to the Huang−Rhys factor ($S$), which is the intensity ratio of the first vibrational component to the second component,[21] by the relation $S = {}^1/_2\Delta_q{}^2$, so that $\lambda_v(q) = {}^1/_2\Delta_q{}^2 h\nu(q)$. Another factor that must be considered in analyzing spectra to extract $\lambda_v$ is the "missing mode effect" (MIME) that ensures that the vibrational features observed in the optical spectrum do not correspond to vibrations present in the compound; instead, observed features occur between values of normal modes.[20] Although the region of the spectrum of **$(NO_2)_2$-PH$^-$** showing the three maxima could be fit modestly well using only three modes (1590, 960, and 580 cm$^{-1}$, producing $\lambda_v$ = 1050 cm$^{-1}$, see Supporting Information for details), more modes are doubtless involved. A density functional theory calculation of **$(NO_2)_2$-PH$^-$** at the B3LYP/6-31+G* level gave a very slightly asymmetrical structure with nine modes having the significant nonresonance Raman intensity expected for modes that would contribute to the IV transition (see Table 2, and Supporting Information for more detail). As documented in the Supporting Information, rather similar fits to the region of the three maxima can be obtained with three, four, five, and six modes, chosen to be reasonably close to the calculated modes or averages of them, with $\Delta_q$ values chosen to still fit the spectrum. The fits obtained are certainly not unique, and a good fit could be obtained with other $h\nu_q$,$\Delta_q$ combinations. Furthermore, smaller frequencies can to some extent be incorporated into the damping parameter, $\Gamma$, which is the full width at half-height employed for the components of the spectrum. We found best fit to the low-frequency region by using two modes with frequencies below 900 cm$^{-1}$ and using a relatively small $\Gamma$ value (556 cm$^{-1}$). The five-mode fit for which parameters are shown in Table 2 is compared with the observed spectrum in Figure 10. The only Raman-active C−H stretching mode is also included in Table 2 because it involves a small but noticeable breathing motion of the benzene ring and hence could be involved in the optical transition. Fit to the experimental spectrum is improved by including a small $\Delta_q$ mode near this frequency (see Supporting Information), although the high-energy end of most optical transitions begins to overlap with other bands, so it is not really clear whether a better fit to this region is a good criterion for including high-frequency modes. Inclusion of this CH mode raises the $\lambda_v$ estimate from 989 to 1059 cm$^{-1}$ (see the summary in Table 3). The estimated $\lambda_v$ is relatively insensitive to the number of modes used to fit the spectrum, and we include only two fits for each in Table 3, one with high-frequency modes and one without. The optical spectrum of **$(NO_2)_2PH^-$** is therefore consistent with a vibrational reorganization energy for the IV transition of this Class III IV compound of 990−1060 cm$^{-1}$, comparable to those calculated for formation of acene radical cations (about 1100 cm$^{-1}$ for anthracene, 910 for tetracene, and 800 for pentacene).[19] The value of $2H_{ab}/\lambda$ for **$(NO_2)_2PH^-$** is therefore estimated at over 10, making it only slightly smaller than the value of 11.6 obtained from the resonance Raman study of the *p*-phenylenediamine derivative **$(k33N)_2PH^+$**.[11] Despite slightly stronger

(19) Coropceanu, V.; Malagoli, M.; da Silva Filho, D. A.; Gruhn, N. E.; Bill, T. G.; Brédas, J.-L. *Phys. Rev. Lett.* **2002**, 275503.
(20) Zink, J. I.; Shin, K.-S. K. Molecular Distortion in Excited Electronic States Determined from Electronic and Resonance Raman Spectroscopy. *Adv. Photochem.* **1991**, *16*, 119.
(21) Brunold, T. C.; Güdel, H. U. Luminescence Spectroscopy. In *Inorganic Electronic Structure and Spectroscopy*; Solomin, E. I., Lever, A. B., P., Eds; Wiley: New York, 1991; Vol. 1, p 259.

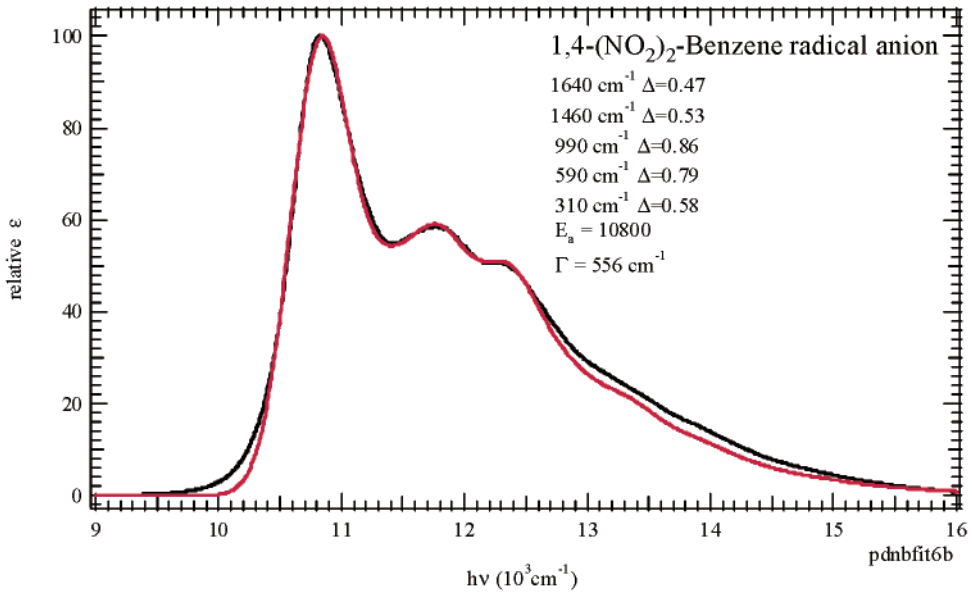


***Figure 10.*** Comparison of the spectrum of **1,4-$(NO_2)_2$-PH**$^-$ (black) with a simulation (red) using the five-mode calculation summarized in Table 2.

***Table 3.*** Summary of $\lambda_v$ Values Obtained from Fitting Optical Spectra of Dinitroaromatic Radical Anions

| bridge | modes | frequencies ($cm^{-1}$) | $\lambda_v$ ($cm^{-1}$) | $G$ ($cm^{-1}$) | $E_{00}$ ($cm^{-1}$) | $2H_{ab}/\lambda_v$ |
|---|---|---|---|---|---|---|
| 1,4-PH | 5 | 1640, 1460, 990, 590, 310 | 989 | 556 | 10800 | 10.9 |
| | 6 | 3200,1640,1460,990,590,310 | 1059 | 556 | 10800 | 10.2 |
| 2,6-NA | 6 | 1630,1470,1060,850,610,310 | 788 | 506 | 8470 | 10.7 |
| | 8 | 3240,2250,1630,1470,1060,850,610,310 | 888 | 506 | 8470 | 9.5 |
| 2,6-AN | 6 | 1600,1470,1060,850,610,310 | 738 | 559 | 7340 | 9.9 |
| | 8 | 3000,2160,1600,1470,1060,830,610,310 | 872 | 559 | 7340 | 8.5 |
| 2,7-$M_2$- | 6 | 1660,1150,940,670,550,300 | 992 | 639 | 6760 | 6.8 |
| -FL | | 3000,2200,1650,1160,940,570,550,300 | 1286 | 666 | 6760 | 5.3 |
| 4,4′-BI | 6 | 1640,1490,1110,850,610,310 | 1216 | 849 | 6770 | 5.6 |
| | 8 | 3240,2310,1640,1490,1110,850,610,310 | 1919 | 849 | 6770 | 3.5 |
| 1,5-NA | 5 | 1610, 1430, 980, 610,310 | 912 | 994 | 6690 | 7.3 |
| | 7 | 3250,2200,1620,1430,980,610,310 | 1163 | 1016 | 6700 | 5.6 |

delocalization, the optical spectrum of **(k33N)$_2$PH**$^+$ shows less resolution, presumably because of more modes contributing in the presence of the 21-atom dialkylamino **M** unit than for the three-atom nitro one. The combination of larger line width caused by smaller $2H_{ab}/\lambda$ and more active modes caused by the 31-atom dianisylamino **M** group causes the broad envelope observed for **1,4-Da$_2$PH**$^+$ absorption (Figure 2).

The vibrational structures observed for **2,6-$(NO_2)_2$ NA**$^-$ and **2,6-$(NO_2)_2$ AN**$^-$ are rather similar to that of their **PH** analogue, although the maximum observed near 950 $cm^{-1}$ decreases in importance, and the $\lambda_v$ estimated from the fitting parameters drops, but not as much as $H_{ab}$, so that $2H_{ab}/\lambda_v$ decreases as aryl bridge size increases. The spectra of **2,7-$(NO_2)_2$-M$_2$FL** and **4,4′-$(NO_2)_2$-BI**$^-$ are noticeably broader than those of the other cases and require a larger Γ for their fit. Their $2H_{ab}/\lambda_v$ values are also significantly smaller. It appears that Γ increases significantly as $H_{ab}/\lambda_v$ approaches the Class II, Class III borderline value of 1, although other factors may be involved in determining the Γ required for fitting.

The value of $\lambda_v$ obtained from the fit is larger for **1,5-$(NO_2)_2$-NA**$^-$ than for its 2,6-isomer, which might be caused by twisting the $C_{Ar}-NO_2$ bonds in this more hindered compound; AM1 calculations optimize the 1,5-isomer with the $NO_2$ group twisted 10.6° out of the ring plane. **4,4′-$(NO_2)_2$-BI**$^-$ has an even larger $\lambda_v$, which we suggest is probably a result of the twisting mode about the central CC bond, a structural feature not present in the other compounds. Miller, Closs, and co-workers have discussed the importance of such torsional motion, to which they attribute a $\lambda_v$ increment of about 1050 $cm^{-1}$ when biphenyl is a charge-bearing unit in their $\sigma$-bond-bridged quinone, biphenyl systems.[22]

## Summary

Dinitroaromatic radical anions of the Kekule substitution pattern are delocalized (Class III) IV compounds, as demonstrated by the vibrational fine structure observed in their near-IR absorption bands. Their electronic couplings ($H_{ab}$) decrease as expected as the number of bonds between the nitrogen atoms increase for the bridges **1,4-PH** (five bonds), **2,6-NA** (seven bonds), **2,6-AN** (nine bonds), but the five-bond **1,5-NA** system has a smaller electronic coupling than all of these systems. It is about the size expected when counting the 11 bonds around the C═C−C periphery instead of across the formally single-bonded five-bond pathway. The ET distances on the hypothetical diabatic surfaces ($d_{ab}$) obtained from the transition dipole moments using generalized Mulliken−Hush theory are 26−40% of the N,N distances. The physical significance of these numbers is not obvious, but the nitro-substituted radical anions show much smaller $d_{ab}$ at comparable $H_{ab}$ than do IV radical cations.

(22) Miller, J. R.; Paulson, B. P.; Bal, R.; Closs, G. L. *J. Phys. Chem.* **1995**, *99*, 6923.

***Table 4.*** Summary of Band Maxima for Delocalized $(NO_2)_2Ar^-$

| bridge | $h\nu_{max}$ ($cm^{-1}$) | $\epsilon_{max}$ ($M^{-1}cm^{-1}$) | $\Delta h\nu$ ($cm^{-1}$) | $\epsilon$ ratio |
|---|---|---|---|---|
| 1,4-PH | 10820 | 20300 | – | – |
| | 11750 | 11910 | 930 | 0.59 |
| | 12270 | 10250 | 1450 | 0.50 |
| 2,6-NA | 8500 | 55200 | – | – |
| | 9470 | 19460 | 970 | 0.35 |
| | 10050 | 19860 | 1550 | 0.36 |
| 2,6-AN | 7380 | 39870 | – | – |
| | 8900 | 14320 | 1520 | 0.36 |
| 9,9-$Me_2$ | 6790 | 16470 | – | – |
| FL | 8365 | 9257 | 1575 | 0.56 |
| 4,4′-BI | 6900 | 9920 | – | – |
| | 8440 | 8480 | 1540 | 0.85 |
| 1,5-NA | 6800 | 6380 | | |
| | 8120 | 4030 | 1320 | 0.63 |

The dinitroaryl radical anion IV bands show good enough vibrational resolution to extract estimated $\lambda_v$ values, which are about 1000 $cm^{-1}$ for the **PH**-bridged system and decrease as bridge size is increased for **1,4-PH**, **2,6-NA**, and **2,6-AN** bridges. The $\lambda_v$ is larger for both the **1,5-NA**-bridged compound (twisted at the $C_{Ar}-NO_2$ bonds) and the 4,4′-BI-bridged one (twisted at the central bond), and their intrinsic line widths (as represented by the $\Gamma$ fitting parameter) are also larger.

## Experimental Section

Commercial 1,4-dinitrobenzene was purified by elution with toluene from a short column packed with alumina, followed by recrystallization from ethanol. 2,6-Dinitronaphthalene was kindly supplied by G. Grampp. The 2,6-dinitronaphthalene was prepared from commercially available 2,6-dihydroxynaphthalene (EGA-Chemie, Germany) by treating it with aqueous ammonia in an autoclave forming the 2,6-diaminonaphthalene, which was then oxidized to the final dinitronaphthalene[23] (mp 278 °C, lit.[23b] 279 °C). 2,6-Dinitroanthracene was prepared by pyrolysis of a mixture of 2,6- and 2,7-dinitro-9,10-ethano-9,10-dihydroanthracene[24] and separated from the 2,7-dinitro isomer by a combination of column chromatography and fractional recrystallization from chlorobenzene, mp >300°; *m/z* 268 ($M^+$); $^1H$ NMR (300 MHz; DMSO-$d_6$) $\delta$ 9.28 (s, $2H_{1,4}$), 9.20 (s, $2H_{9,10}$), 8.42 (d, $2H_{3,6}$ $J$ = 9.3 Hz), 8.42 (d, $2H_{4,8}$ $J$ = 9.3 Hz). 4,4′-Dinitrobiphenyl was prepared by deamination of commercial 4,4′-dinitro-2-biphenylamine, mp = 239−240 °C (lit.[25] 239 °C).

The radical anions were prepared in vacuum-sealed glass cells equipped with an ESR tube and a quartz optical cell. Reduction was achieved by contact with 0.2% Na−Hg amalgam. The nitro compound, a 100-fold excess of commercial cryptand, and the Na−Hg amalgam were introduced in different chambers of the cell under nitrogen. The cryptand was degassed by melting under high vacuum before addition of DMF. The concentration of the samples was determined spectrophotometrically before reduction. UV/vis/NIR spectra were recorded at room temperature with a Shimadzu 3101 PC spectrometer at several stages of reduction, so that the radical anion oxidation level spectrum could be selected.

The observed optical band positions and maxima are summarized in Table 4.

We evaluated $\mu_{12}$ using Liptay's formulation of the integral over the absorption band (eq 1).[26]

$$|\mu_{12}| = N\left(\frac{1000\ln(10)3hc}{8\pi^3 N_A}\int_{band}\frac{\epsilon(\bar{\nu})}{\bar{\nu}}d\bar{\nu}\right)^{1/2} = N0.09584\left(\int_{band}\frac{\epsilon(\bar{\nu})}{\bar{\nu}}d\bar{\nu}\right)^{1/2} \quad (1)$$

It allows evaluation of bands showing fine structure, which cannot be done properly using the more common formulation that puts the wavenumber ($\bar{\nu}$) divisor outside the integral or Hush's simple formula for Gaussian-shaped bands.[7a] The constant given is that required for evaluation of $\mu_{12}$ in Debye using $\bar{\nu}$ in $cm^{-1}$. We also include in eq 1 the solvent refractive index ($n$) correction, $N$ (eq 2), to $\epsilon$ that was first incorporated into interpreting ET using optical analysis by the Kodak group.[27]

$$N = \frac{3\sqrt{n}}{(n^2+2)} \quad (2)$$

The DFT calculation used the Gaussian program,[28] the band integrations using eq 1 were done with software written by A.E.K., and the spectral simulations including vibrational fine structure (Table 3, Figure 10, and Supporting Information) were done with program abs/emis/Raman, obtained from J. I. Zink, which is based on a time-dependent Hamiltonian spectral analysis.[20]

**Acknowledgment.** We thank the National Science Foundation for financial support through Grants CHE-9988727 and CHE-0240197 (S.F.N.) and the Portuguese F.C.T through I.S.T-Centro de Processos Químicos and PRAXIS/2/2.1/QUI/306/94 Project (J.P.T.). We thank Günter Grampp (Techn. Univ. Graz) for supplying the 2,6-dinitronaphthalene sample employed. We thank Jeffrey Zink (UCLA) for supplying his program abs/emis/Raman and his graduate students Susan Baily and Jenny Lockhard for benchmarks and preliminary calculations.

**Supporting Information Available:** **1,4-$(NO_2)_2$-$PH^-$** B3LYP/6-31+G* vibrations and displacement vector pictures for the Raman-active bands, six calculated fits for the **1,4-$(NO_2)_2$-$PH^-$** spectrum, and the fits corresponding to the other entries in Table 3 (PDF). This material is available free of charge via the Internet at http://pubs.acs.org.

JA036066M

(23) (a) Chatt, L.; Wayne, W. P. *J. Chem. Soc., Perkin Trans. 1* **1946**, 33. (b) Vesely, V.; Jakes, M. *Bull. Soc. Chim. France* **1923**, *33*, 942.
(24) Tanida, H.; Ishitobi, H. *Tetrahedron Lett.* **1964**, *15*, 807.
(25) Gull, H. C.; Turner, E. E *J. Chem. Soc.* **1929**, 491.
(26) Liptay, W. *Angew. Chem., Int. Ed. Engl.* **1969**, *8*, 177.
(27) (a) Gould, I. R.; Noukakis, D.; Gomez-Jahn, L.; Young, R. H.; Goodman, J. L.; Farid, S. *Chem. Phys.* **1993**, *176*, 439. (b) Gould, I. R.; Young, R. H.; Albrecht, A. C.; Mueller, J. L.; Farid, S. *J. Am. Chem. Soc.* **1994**, *116*, 8188. (c) Although the Kodak group first used a larger factor[a] they very soon argued that the smaller factor shown in (3) is a better one to use,[b] but also cautioned that the true solvent effect is proably more complex.
(28) Frisch, M. J.; Trucks, G. W.; Schlegel, H. B.; Scuseria, G. E.; Robb, M. A.; Cheeseman, J. R.; Zakrzewski, V. G.; Montgomery, J. A. J.; Stratmann, R. E.; Burant, J. C.; Dapprich, S.; Millam, J. M.; Daniels, A. D.; Kudin, K. N.; Strain, M. C.; Farkas, O.; Tomasi, J.; Barone, V.; Cossi, M.; Cammi, R.; Mennucci, B.; Pomelli, C.; Adamo, C.; Clifford, S.; Ochterski, J.; Petersson, G. A.; Ayala, P. Y.; Cui, Q.; Morokuma, K.; Malick, D. K.; Rabuck, A. D.; Raghavachari, K.; Foresman, J. B.; Cioslowski, J.; Ortiz, J. V.; Baboul, A. G.; Stefanov, B. B.; Liu, G.; Liashenko, A.; Piskorz, P.; Komaromi, I.; Gomperts, R.; Martin, R. L.; Fox, D. J.; Keith, T.; Al-Laham, M. A.; Peng, C. Y.; Nanayakkara, A.; Gonzalez, C.; Challacombe, M.; Gill, P. M. W.; Johnson, B.; Chen, W.; Wong, M. W.; Andres, J. L.; Gonzalez, C.; Head-Gordon, M.; Replogle, E. S.; Pople, J. A. *Gaussian 98*, Revision A.7; Gaussian, Inc.: Pittsburgh, PA, 1998.